J. Plasma Fusion Res. SERIES, Vol. 6 (2004) 622–625

Orbit Topology and Confinement of Energetic Ions in the CHS-qa Quasi-Axisymmetric Stellarator

ISOBE Mitsutaka, NAKAJIMA Noriyoshi, SHIMIZU Akihiro, SUZUKI Chihiro, AKIYAMA Tsuyoshi, NISHIMURA Shin, OKAMURA Shoichi, MATSUOKA Keisuke and SPONG Donald A.[1]

National Institute for Fusion Science, Toki, 509-5292, Japan

[1]Oak Ridge National Laboratory, P.O.Box 2009, Oak Ridge, TN 37831-8072, U.S.A.

(Received: 10 December 2003 / Accepted: 24 May 2004)

Abstract

The orbit topology and confinement of neutral beam-injected energetic ions are investigated for the current target configuration of the CHS-qa quasi-axisymmetric stellarator. It was shown that tangentially co-injected neutral beam (NB) heating is efficient even at a low magnetic field strength B_t of 0.5 T, whereas the heating efficiency of the counter-injected NB becomes significantly lower as B_t decreases because of the increase of first orbit loss. The energy loss rate increases as the beam injection angle becomes perpendicular, suggesting that the residual non-axisymmetric ripple in the peripheral domain plays a role in enhancing the transport of trapped ions. An interesting observation involves the appearance of the island structure in both the gyro motion following orbit and the guiding center collisionless orbit of counter-moving transit beam ions. It appears under a particular, narrow range of parameters, i.e., energy, pitch angle $v_{//}/v$, normalized minor radius r/a at the launching point and B_t.

Keywords:

quasi-axisymmetric stellarator, non-axisymmetric magnetic field ripple, neutral beam, energetic ion, orbit, heating efficiency

1. Introduction

The quasi-axisymmetric stellarator CHS-qa, which is one of the so-called advanced stellarators, has been designed to provide a high level of neoclassical confinement as well as magneto-hydrodynamic (MHD) stability while realizing a tokamak-like, toroidally symmetric magnetic structure in Boozer coordinates [1-4]. In the CHS-qa, the neoclassical transport is significantly improved compared with that in the existing CHS [5,6]. However, we must verify the orbits and confinement property of energetic ions since residual non-axisymmetric magnetic field components exist in the edge region and these residual ripples can enhance the radial diffusion of toroidally trapped energetic ions. The effect of residual ripples on barely passing energetic ion orbits is also of interest because their orbits may become stochastic over many toroidal circulations and finally escape from the system. In the present study, the orbit topology of collisionless beam ions is numerically studied for the CHS-qa configuration in both Cartesian and Boozer coordinates. The global confinement property of neutral beam (NB)-injected energetic ions is also investigated by use of particle simulation code DELTA5D following the guiding center orbits in the presence of slowing-down and pitch angle scattering processes on Boozer coordinates.

2. CHS-qa with quasi-axisymmetry

First, the basic features of the current target configuration of the CHS-qa are briefly described. The CHS-qa has toroidal periods of 2, and a fairly low aspect ratio of 3.2. Figure 1a shows poloidal cross sections with three different toroidal angles ϕ. The rotational transform $\iota/2\pi$ ranges from 0.355 to 0.385 in the vacuum (see Fig.1b) and increases as β increases because of co-flowing bootstrap current [7]. The equilibrium magnetic field is characterized by a B_{10}(toroidicity)-dominated magnetic field structure in the system's entire region although residual helical magnetic field ripples still exist in the peripheral region as seen in Fig. 1c. The magnetic well is formed in the plasma's entire region, and its depth is about 5 % at the boundary. The average major radius R_{ave} and the magnetic field strength B_t of the CHS-qa are 1.5 m and 1.5 T, respectively, in the present design [3].

3. Orbit topology

3.1 Collisionless orbits of parallel and anti-parallel beam ions

Assuming a tangential NB injection, which will be one of the primary heating methods for real experiments, the collisionless orbits of parallel and anti-parallel NB ions are

Corresponding author's e-mail: isobe@nifs.ac.jp

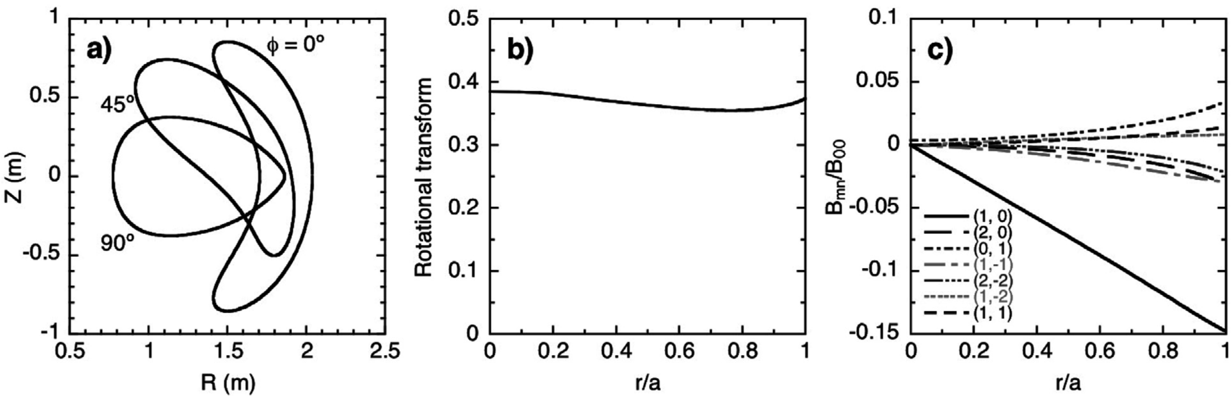

Fig. 1 (a) Poloidal cross sections of the CHS-qa for different toroidal angles ϕ. (b) Radial profile of rotational transform in vacuum equilibrium. (c) Radial profile of the magnetic field spectrum.

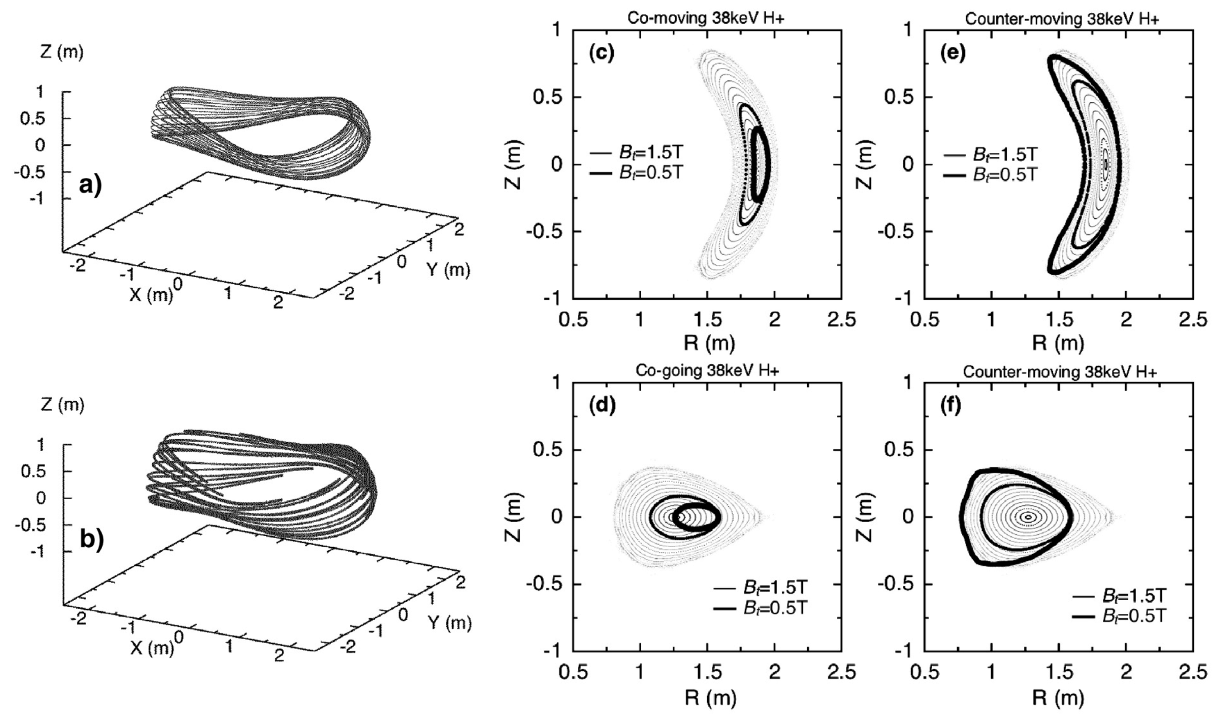

Fig. 2 Collisionless beam ion orbits in Cartesian coordinates for CHS-qa. (a) Three-dimensional plots of typical orbits of energetic passing H+ ions ($v_{//}/v$ ~ 1), and (b) toroidally trapped ($v_{//}/v$ ~ 0.26) ions with an energy of 38 keV in B_t of 1.5 T. Poincaré plots of co-moving (c,d) and counter-moving (e,f) transit beam ions at ϕ = 0° (c,e) and ϕ = 90° (d,f) cross sections. The gray and black lines represent orbits at B_t of 1.5 T and 0.5 T, respectively. Both ions are launched at R = 1.95 m on the equatorial plane of the ϕ = 0° cross section.

investigated. In the CHS-qa, the orbits of confined particles are classified into two types, i.e., passing and toroidally trapped. Figures 2a and 2b show three-dimensional plots of typical passing and toroidally trapped orbits of energetic ions in Cartesian coordinates by following full gyro motions in the vacuum magnetic field produced by 20 modular coils for B_t of 1.5 T [8]. Particle orbits in CHS-qa are quite similar to those in tokamak. Helically trapped orbits, which play an important role in energetic ion transport in a conventional system like CHS, are not seen in the CHS-qa. In order to determine to what degree the orbit of the transit beam ion deviates from magnetic flux surfaces, Poincaré plots of co- and counter-moving ions with energy E of 38 keV, which is an injection energy E_b of existing NB injector of CHS, at ϕ = 0° (bean-shaped cross section) and ϕ = 90° (horizontally elongated cross section) are shown for different B_t in Figs. 2c-f. Beam ions are launched with $v_{//}/v$ ~ ±1 corresponding to parallel and anti-parallel injection at major radius R = 1.95 m (r/a ~ +0.53) on the equatorial plane of the ϕ = 0° cross section. Here, "+" in r/a stands for the large R side distant from the magnetic axis. The thin black and thick gray lines represent orbits at B_t of 1.5 T and 0.5 T in the absence of collisions, respectively. Orbit analysis shows that the co-moving beam ions whose birthplaces are in the large R side are well confined, as expected. Although the beam ion orbits deviate substantially from the magnetic flux surfaces at B_t of 0.5 T as seen in Figs. 2c and 2d, beam ions remain inside the system even if they are born in a further peripheral region at the large R side. On the other hand, counter-injected beam ions ionized at the edge region will be promptly lost even without collisions because their orbits largely deviate from the flux surfaces toward the inboard side and then cross the last closed magnetic flux surface (see Figs. 2e and 2f). Orbit analysis indicates that NB ions ionized at $R > 1.93$ m ($r/a \gtrsim +0.45$) can escape promptly at B_t of 0.5 T, suggesting that counter-injected NB heating will not be as efficient. By increasing B_t, the first orbit loss domain of counter-injected beam ions becomes narrower, as expected, and the confinement/first orbit loss boundary is now located at R = 1.99 m ($r/a \sim +0.75$) in B_t of 1.5 T. The first orbit loss rate of counter-moving beam ions will not be serious in B_t of 1.5 T because a deposition rate of NB ions in the peripheral region is expected to be small.

3.2 On island structure

With regards to the energetic ion orbits in CHS-qa, an interesting observation involves the appearance of the island structure on the beam ion orbit. In the beginning of this work, we found an island structure with a poloidal mode number m = 6 on gyro motion following orbits of counter-moving transit beam ions in the vacuum magnetic field obtained from modular coils in a particular parameter range. In order to clarify whether the island in the orbit is due to resonance between gyro motion and the variation of magnetic field, guiding center orbits were investigated. Figure 3 shows the Poincaré plot of the guiding center orbit for counter-passing ion of E = 38 keV in the equilibrium magnetic field having B_t of 1.0 T. The equilibrium magnetic field is obtained from the three-dimensional MHD equilibrium code VMEC [9] which is then transformed to Boozer coordinates. The island

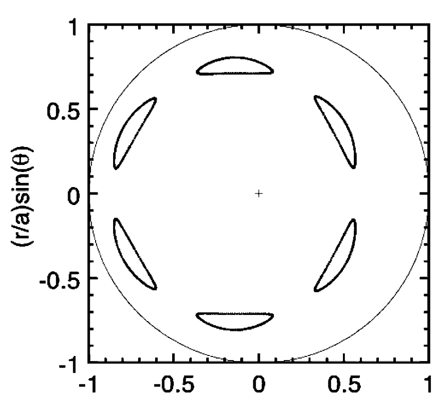

Fig. 3 Island structure appearing on the Poincaré plot at $\phi = 0°$ with n/m = 2/6 of the guiding center orbit of the counter-moving transit beam ion in Boozer coordinates. Energy and $v_{//}/v$ are 38 keV and 0.63, respectively. The ion is launched at r/a = 0.61 at the equatorial plane of ϕ = 90°.

with m = 6 appeared again, although there is no magnetic island in this field because nested flux surfaces are assumed in VMEC. The toroidal mode number n was 2 in this case. Because of the appearance of the island structure even in the guiding center orbit, it can be now stated that this island is not due to the resonance effect coming from the gyro motion. It is important to note that $\iota/2\pi$ of the magnetic field does not contain a resonance of n/m = 2/6 and is always higher than this. The appearance of the island structure is sensitive to parameters such as $v_{//}/v$, E, and r/a at the launching point of energetic ions and is especially very sensitive to B_t. The island seen in Fig. 3 appears in the following narrow parameter ranges, i.e. B_t = 1.0 T, $0.61 < v_{//}/v < 0.64$, 36 keV $< E <$ 38 keV, and $0.58 < r/a < 0.61$. The low m island structure in the orbit has never been seen so far for co-moving transit beam ions. Efforts to understand the mechanism of island formation in an orbit are being made.

4. Simulation of beam ion confinement in the presence of collisions by using DELTA5D

In an evaluation of NB ion confinement, it is important to consider the slowing-down and pitch angle scattering processes of beam ions because the beam ions may be scattered into unconfined orbits through collisions with bulk plasma. In order to evaluate global beam ion confinement in the presence of collisions, the particle simulation code DELTA5D [10] was employed. The guiding center beam ion orbits are tracked in the equilibrium magnetic field obtained from the VMEC code which are then transformed to Boozer coordinates. The beam ions slowed down to $(3/2)T_i$ are counted as part of thermal ions. The plasma parameters used here are $n_e(0) = 6.0 \times 10^{19}$ m^{-3} with a profile of $n = n(0)\cdot[1 - (r/a)^2]$, and $T_e(0) = T_i(0)$ = 1.5 keV with a profile of $T = T(0)\cdot[1 - (r/a)^2]^2$. n_i (hydrogen) is given as $0.91n_e$ and one impurity component is considered. The plasma potential is not considered here. An NB of 38 keV is injected into the plasma on the equatorial plane of the $\phi = 0°$ cross section and the initial pitch angle is given by taking the ratio of the tangency radius R_{tan} of the NB to the local value of R where the particles are ionized. The profile of the NB ion density n_b is assumed to be as $n_b = n_b(0)\cdot[1 - (r/a)^2]$, and only magnetic flux surfaces having $R > R_{ax}$ are populated with beam ions. Here, R_{ax} represents the magnetic axis position. Currently, the charge exchange loss of beam ions is not considered in this analyis. Figure 4 shows the time evolution of the percentage of energy lost ($\langle E \rangle$ lost) from the beam averaged over the ensemble of 1,000 ions, the number of confined ions, and the averaged energy of ions in volume averaged magnetic field strength $\langle B \rangle$ of 1.5 T with R_{tan} = 1.85 m, corresponding to the parallel injection. The percentage of $\langle E \rangle$ lost is determined when it reaches a saturated plateau in its time evolution ; this plateau is associated with the average beam ion decelerating to the energy level of $(3/2)T_i$. $\langle E \rangle$ lost is evaluated to be 9.5 % in this case. The energy of escaping beam ions is characterized by a broad peak centered around 10 keV as seen

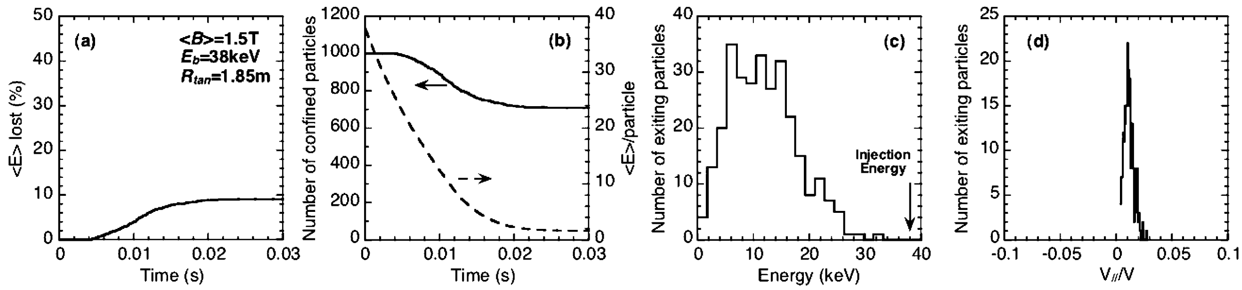

Fig. 4 (a) Time evolution of ⟨E⟩ lost (%), (b) Number of confined ions and ⟨E⟩/ions in the vacuum equilibrium, Number of exiting beam ions as a function of energy (c) and pitch angle $v_{//}/v$ (d).

in Fig. 4c. The pitch angle distribution is very peaked around the deeply trapped range (see Fig. 4d).

We have studied the dependence of ⟨E⟩ lost on R_{tan} and B. The energy loss rate increases as R_{tan} becomes small (see Fig. 5a). Concerning tangential co-injection, the ⟨E⟩ lost is about 9.5 % at R_{tan} of 1.85 m and increases to 25 % at R_{tan} of 1.25 m. The primary reason for this tendency is a radial diffusion of beam ions through ripple trapping due to pitch angle scattering. Because the initial beam ion orbits are closer to the passing-trapped boundary in velocity space as R_{tan} is decreased, they can be trapped more easily. Residual ripples appear to play an important role in the confinement of toroidally trapped beam ions. The loss rate of counter-injected beam ions is higher than that in co-injected ions, as expected, and this is mainly due to prompt, first orbit loss. Next, by keeping R_{tan}, the variation of ⟨E⟩ lost in relation to ⟨B⟩ is investigated. The ⟨E⟩ lost of counter-injected beam ions strongly depends on the magnitude of ⟨B⟩ and increases to 40 % even in tangential injection because of a significant first-orbit loss fraction, whereas ⟨E⟩ lost of the co-injected NB ions is not significantly sensitive to the magnitude of ⟨B⟩.

5. Summary

We have studied the orbit topology and confinement of NB-injected energetic ions for the current target configuration of the CHS-qa. It appears that tangentially co-injected beam ions are well confined even in the presence of collisions, and ⟨E⟩ lost is evaluated to be about 9.5 % at B_t of 1.5 T. However, the beam ion confinement deteriorates as R_{tan} decreases because of the existence of residual non-axisymmetric magnetic field ripples that enhance the radial diffusion of toroidally trapped ions. As ⟨B⟩ decreases, the confinement of counter-injected NB ions tends to be worse than that of co-injected ions due to a fraction of first orbit loss, and ⟨E⟩ lost is evaluated to be about 40 % at ⟨B⟩ of 0.5 T.

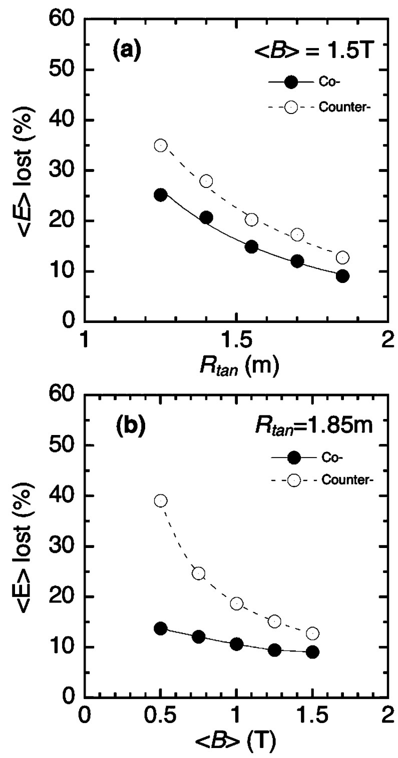

Fig. 5 (a) Dependence of beam ion losses on R_{tan} in ⟨B⟩ of 1.5 T. (b) Dependence of beam ion losses on field strength in R_{tan} of 1.85 m in the vacuum equilibrium.

References

[1] K. Matsuoka *et al.*, Plasma Phys. Rep. **23**, 542 (1997).
[2] S. Okamura *et al.*, J. Plasma Fusion Res. SERIES **1**, 164 (1998).
[3] S. Okamura *et al.*, Nucl. Fusion **41**, 1865 (2001).
[4] K. Matsuoka *et al.*, J. Plasma Fusion Res. SERIES **4**, 111 (2001).
[5] M.F. Heyn *et al.*, Plasma Phys. Control. Fusion **43**, 1311 (2001).
[6] V.V. Nemov *et al.*, Plasma Phys. Control. Fusion **45**, 1829 (2003).
[7] M. Isobe *et al.*, J. Plasma Fusion Res. SERIES **5**, 360 (2002).
[8] A. Shimizu *et al.*, Fusion Eng. Des. **65**, 109 (2003).
[9] S.P. Hirshman and J.C. Whiton, Phys. Fluids **26**, 3553 (1983).
[10] H. Kugel *et al.*, *to be published in* Fusion Sci. Technol.